ChemPubSoc Europe

DOI: 10.1002/cplu.201402329

CHEMPLUSCHEM Full Papers

Synthesis and Characterization of a Biotinylated Multivalent Targeted Contrast Agent

Serhat Gündüz,[a, b] Anthony Power,[b] Martin E. Maier,[c] Nikos K. Logothetis,[b, d] and Goran Angelovski*[a]

A new bimodal and multivalent dendritic contrast agent (CA) that targets the protein avidin was prepared and characterized. The tripartite lysine core was used to link the ligand biotin, the fluorescent dye, and the dendron carrying GdDOTA (DOTA = 1,4,7,10-tetraazacyclododecane-1,4,7,10-tetraacetic acid) chelates for amplification of the magnetic resonance imaging (MRI) signal. The longitudinal relaxivity of this dendrimeric CA was greater than those of its GdDOTA chelate and most of the common commercial agents at the investigated high magnetic field (7 T). The capacity of the dendrimeric CA to bind to the target protein was confirmed by fluorescence measurements upon its treatment with NeutrAvidin–agarose gel or NeutrAvidin-coated microspheres and the results were compared with those of its monomeric analogue. The fluorescence intensity of monomer-treated targets was found to be greater than that from those treated with dendrimeric CA; however, a several-fold increase in the MRI signal was observed on the same samples treated with the dendrimeric CA. The inductively coupled plasma mass spectrometry analysis of the digested samples indicated somewhat higher Gd^{3+} content and hence slightly better binding of monomeric versus dendrimeric CA. This bimodal and multivalent targeted probe opens an avenue for the preparation of new nanosized CAs that allow high-resolution MRI of various targets, such as cellular receptors or specific cellular populations.

Introduction

Magnetic resonance imaging (MRI) is a powerful diagnostic and research tool that allows three-dimensional visualization of living tissues at sub-millimeter resolutions. It offers excellent soft-tissue contrast, allowing functionally relevant distinctions between structures in the brain or other organs. Still, many other important structures do not possess sufficient intrinsic contrast to be discriminated from neighboring tissue. Methods to enhance contrast in the local vicinity of specific structures are needed.

MRI contrast can be enhanced by the introduction of exogenous small-molecule contrast agents (CAs).[1] The most frequently employed are chelates of the paramagnetic lanthanide-metal ion gadolinium.[2] These agents shorten the spin–lattice or longitudinal relaxation time (T_1) of water protons in a concentration-dependent manner, and are widely used in clinical diagnostics and experimental research. However, the available monomeric CAs have certain limitations. Typical low-molecular-weight Gd chelates (e.g., 1,4,7,10-tetraazacyclododecane-1,4,7,10-tetraacetic acid (DOTA), diethylenetriamine pentaacetic acid (DTPA)) diffuse rapidly through the extracellular space and distribute in tissues nonspecifically.[1c, 3] Furthermore, relatively high amounts of Gd^{3+} ions need to be localized to the area of interest. Various studies suggest a detection limit of approximately 10^7 Gd^{3+} ions per cell for receptor- or cell-labeling approaches.[4] The need for high local concentrations of CA, combined with its rapid diffusion and elimination from the area of interest, makes it very difficult to visualize specific targets with standard approaches.

The development of targeted CAs that recognize and bind specific biomolecules with high affinity could dramatically increase their local concentration and tissue retention time.[5] To improve detection, the contrast of a cell-targeting CA could be amplified by equipping it with a greater number of Gd^{3+} ions. Targeted CAs with enhanced contrast-generating potential would be valuable for diagnostic studies at the cellular and molecular level. In neuroimaging, they would be of particular use for imaging specific components of complex brain networks undergoing experience-dependent, developmental, or pathological changes.[6] Increasingly, multimodal imaging agents that can be detected by both optical and magnetic res-

[a] Dr. S. Gündüz,[+] Priv.-Doz. Dr. G. Angelovski
MR Neuroimaging Agents Group
Max Planck Institute for Biological Cybernetics
72076 Tübingen (Germany)
E-mail: goran.angelovski@tuebingen.mpg.de

[b] Dr. S. Gündüz,[+] Dr. A. Power,[+] Prof. Dr. N. K. Logothetis
Department for Physiology of Cognitive Processes
Max Planck Institute for Biological Cybernetics
72076 Tübingen (Germany)

[c] Prof. Dr. M. E. Maier
Institute for Organic Chemistry
Faculty of Science, University of Tübingen
72076 Tübingen (Germany)

[d] Prof. Dr. N. K. Logothetis
Department of Imaging Science and Biomedical Engineering
University of Manchester
Manchester M13 9PT (UK)

[+] These authors contributed equally to this work.

Supporting information for this article is available on the WWW under http://dx.doi.org/10.1002/cplu.201402329.

onance (MR) methods are sought after, which extends the spatial scale of imaging into the cellular and subcellular range.

Herein, we report the development of a multimodal CA that accomplishes a twofold goal. First, it targets a protein-based receptor with a very high binding affinity. Second, it follows a strategy designed to improve detection of targeted CA by increasing the number of Gd^{3+} chelates per molecule. We have therefore prepared two tripartite, multimodal, and targeted CAs (MT3-CAs). Both consist of a tripartite lysine core, which links the high-affinity targeting ligand biotin to one arm and the optically detectable fluorescein isothiocyanate (FITC) moiety to another. The third arm carries either a single, monomeric Gd^{3+} chelate (**mMT3-CA**) or multiple Gd^{3+} chelates linked through a dendrimeric carrier (**dMT3-CA**). The biotin ligand was incorporated as it binds to the protein avidin with one of the highest affinities of any known small-molecule–protein interaction.[7] FITC is a fluorescent dye commonly used for in vitro characterization of novel CAs by means of optical imaging methods.[8] Finally, a highly branched dendrimer capable of carrying up to 32 Gd^{3+} chelates was incorporated, thereby allowing MRI signal amplification.[9]

Two different avidin-displaying targets, agarose beads and polystyrene microspheres, were used to assess specific binding of MT3-CAs. Relaxometric, fluorescence, MRI, and inductively coupled plasma mass spectrometry (ICP-MS) measurements were performed to compare the potential of **mMT3-CA** and **dMT3-CA** as targeted imaging agents.

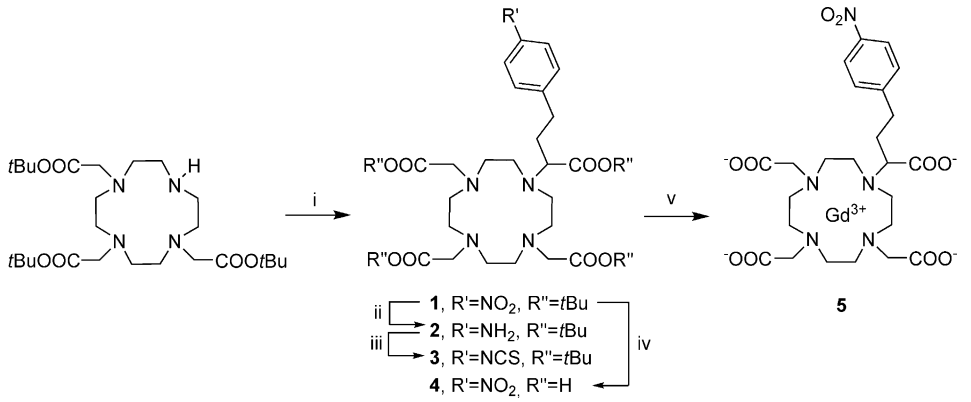

Scheme 1. Synthesis of DOTA-type chelators. Reaction conditions: i) *tert*-butyl 2-bromo-4-(4-nitrophenyl)butanoate, K_2CO_3, DMF, 45 °C, 16 h, 96%; ii) H_2, Pd/C, EtOH, RT, 16 h, 95%; iii) $CSCl_2$, Et_3N, RT, 2 h, 71%; iv) formic acid, 60 °C, 16 h, 94%; v) $GdCl_3 \cdot 6H_2O$, RT, 24 h, 41%.

Results

Synthesis of monomeric and dendrimeric targeted contrast agents

Synthesis of DOTA-type chelators and their Gd^{3+} complexes

To ensure a high stability of the Gd^{3+} complex for application of successive monomeric and dendrimeric CAs, we prepared a DOTA-type chelator linked to an isothiocyanate group that easily reacts with primary amines. The chosen chelator contains four carboxylic groups that form a strong complex with Gd^{3+}, which results in a negatively charged complex, an advantageous property in terms of water solubility and the overall charge of the dendrimeric targeted CA.

Preparation of the desired chelator started from tri-*tert*-butyl 1,4,7,10-tetraazacyclododecane-1,4,7-triacetate (DO3A-*t*Bu ester), which was alkylated with *tert*-butyl 2-bromo-4-(4-nitrophenyl)butanoate to yield **1** (Scheme 1). The nitro group in **1** was reduced by palladium-catalyzed hydrogenation to give the aniline **2**. The isothiocyanate **3** was finally obtained by conversion of **2** with thiophosgene and was used in further synthetic procedures for obtaining monomeric and dendrimeric CAs.[10] For comparison, a Gd^{3+} complex of the chelator bearing the nitro group was also prepared. In this case the *tert*-butyl esters in **1** were hydrolyzed with formic acid to give the acid **4**, and the complex **5** was prepared by using $GdCl_3 \cdot 6H_2O$ in water (Scheme 1).

Synthesis of monomeric contrast agent

To compare the properties of the dendrimeric CA, we also synthesized an analogous monomeric version **mMT3-CA**, which possesses an identical targeting moiety (D-biotin) and fluorescent dye (FITC). The synthetic route was established starting from lysine as the core molecule, which enables branching in three directions and coupling of three different moieties under various coupling conditions (Scheme 2). N_ε-Boc-L-lysine methyl ester hydrochloride (H-Lys(Boc)-OMe; Boc = *tert*-butoxycarbonyl) was biotinylated using *N'*-(3-dimethylaminopropyl)-*N*-ethylcarbodiimide (EDC) as a coupling reagent to give **6**. To enable FITC coupling through its isothiocyanate group, the methyl ester in **6** was converted to an amide with an excess of ethylenediamine in methanol to result in the primary amine **7**. FITC coupling afforded **8**, whereas the primary amine **9** was prepared from **8** by removing the Boc group using concentrated hydrogen chloride solution in methanol.

The biotin- and FITC-containing intermediate **9** was then used as a starting material in the synthesis of both the monomeric and dendrimeric CAs (see below). For the monomeric CA, the macrocyclic isothiocyanate **3** was directly coupled to **9** in basic medium to give **10**, whereas the *tert*-butyl esters were hydrolyzed with formic acid to afford **11**. Its complexation with Gd^{3+} at neutral pH resulted in **mMT3-CA**, the monomeric CA that was used in the subsequent comparison studies with the dendrimeric analogue.

Synthesis of dendrimeric contrast agent

For the synthesis of a target-specific dendrimeric CA we used the biotinylated intermediate **9** (see above) and a modified

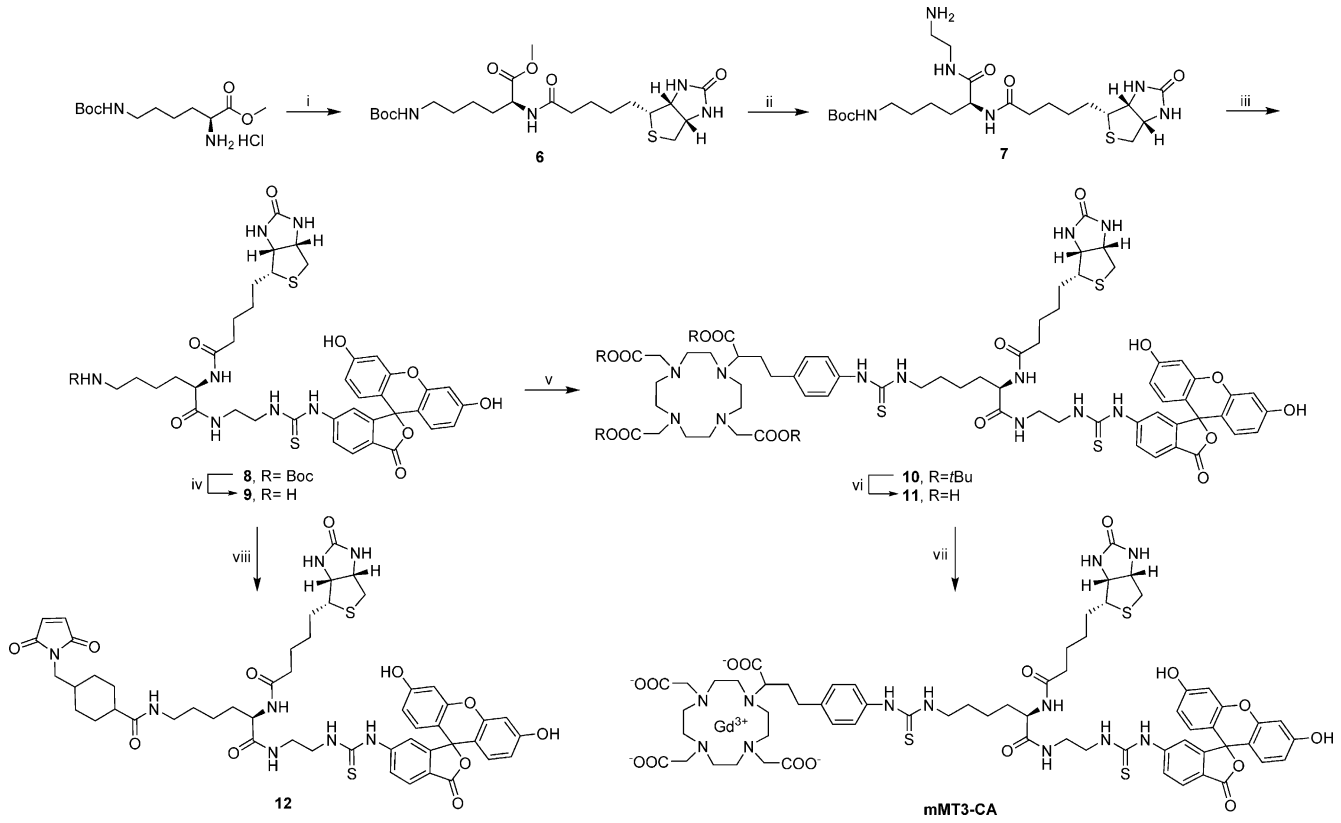

Scheme 2. Synthesis of biotinylated and fluorescently labeled monomeric targeted CA (**mMT3-CA**) and the reactive intermediate **12**. Reaction conditions: i) EDC·HCl, biotin, DMAP, DMF, RT, 48 h, 64%; ii) ethylenediamine, MeOH, RT, 24 h, 77%; iii) FITC, Et_3N, DMF, RT, 16 h, 88%; iv) concd HCl, MeOH, RT, 1 h, 97%; v) **3**, Et_3N, DMF, 45 °C, 16 h, 68%; vi) formic acid, 60 °C, 24 h, 95%; vii) $GdCl_3·6H_2O$, pH 7.0, RT, 24 h, 51%; viii) SMCC, H_2O/DMF, pH 7.5–9.0. DMAP = *N*,*N*-dimethylaminopyridine.

generation 4 (G4) poly(amidoamine) (PAMAM) dendrimer with the cystamine core.[11] The latter allows the controlled coupling of two different functionalities at the dendrimer, the first one through the amino groups on the dendrimer surface, and the second through the sulfhydryl group that can be formed by the reduction of cystamine. This type of dendrimer has already been used for the preparation of biotin–dendrimer conjugates, however with less stable acyclic chelator for Gd^{3+} and a lower dendrimer generation (G2), which ultimately produces lower signal enhancement.[12]

Intermediate **9** was first converted into the sulfhydryl-reactive molecule **12** by coupling it with the succinimidyl-4-(*N*-maleimidomethyl)cyclohexane-1-carboxylate (SMCC) linker.[13] For this purpose, the *N*-hydroxysuccinimide (NHS) ester group in the SMCC linker was reacted with the primary amine in **9** under controlled conditions (pH 7.5 and room temperature) to give **12** (Scheme 2). In parallel, the macrocyclic Gd^{3+} chelators (DOTA) were attached to the amino surface groups of the dendrimer by using previously prepared DOTA-NCS ligand **3**, thus affording dendrimer **13** (Scheme 3). *Tert*-butyl esters in **13** were hydrolyzed using formic acid to give water-soluble dendrimer **14**. Both dendrimer products **13** and **14** were analyzed by matrix-assisted laser desorption/ionization time-of-flight (MALDI-TOF) mass spectrometry (MS) and ^{1}H NMR spectroscopy. MALDI-TOF spectra exhibited broad signals with patterns similar to those previously reported for DTPA-functionalized PAMAM G4 dendrimers.[14] The calculated masses correspond to an average of 37 DOTA chelates per dendrimer molecule, which corresponds to 55–60% conversion of the amino surface groups into the thiourea product with the DOTA-NCS units. The appearance of aromatic protons in the ^{1}H NMR spectra is clear evidence of the DOTA–dendrimer conjugate formation (these peaks do not exist in ^{1}H NMR spectra of the commercial PAMAM G4 dendrimer); however, integration of spectra was less successful than expected,[14] usually indicating a slightly higher amount of DOTA units (when comparing regions of aromatic versus aliphatic protons) than amounts determined by MALDI-TOF.

The disulfide bond in dendrimer **14** was cleaved at pH 7.0 by using tris(2-carboxyethyl)phosphine hydrochloride (TCEP·HCl) to obtain dendron **15** (Scheme 3). To prevent recoupling of the thiol compound, maleimide **12** was immediately added to the reaction mixture.[11] The maleimide group of the SMCC linker reacts with the thiol group of **15** in a slightly acidic medium to give **16**,[13] therefore the pH was maintained at 6.5–7.0 during the reaction. The unreacted dendron **15** was reoxidized by bubbling oxygen gas through the reaction mixture to give dendrimer **14**. The excess amounts of **12** and **14** were removed by using a G-15 Sephadex column and water as eluent. After the purification, the complexation of **16** with $GdCl_3·6H_2O$ at neutral pH resulted in the dendrimeric CA **dMT3-CA**. The excess of Gd^{3+} ions was removed using ethyle-

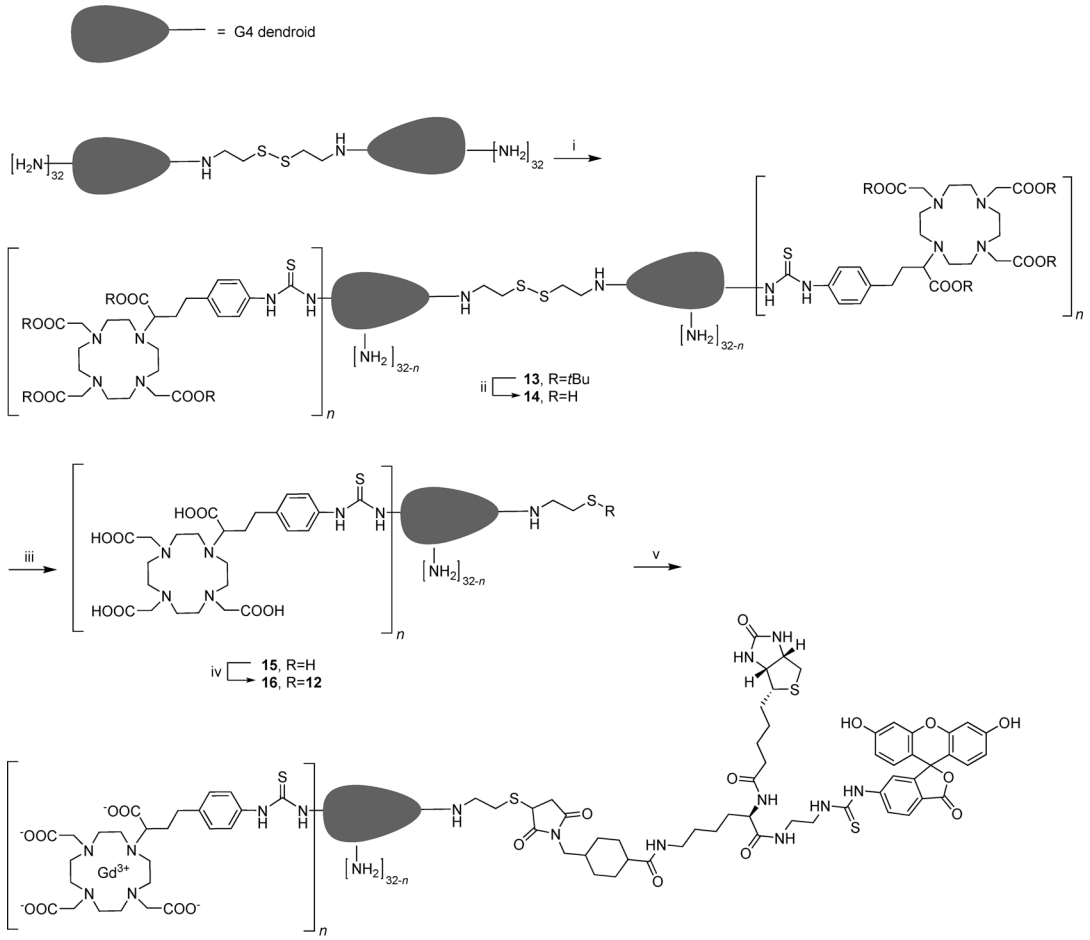

Scheme 3. Synthesis of the dendrimeric MRI CA **dMT3-CA**. Reaction conditions: i) **3**, Et_3N, DMF, 45 °C, 48 h, 81 %; ii) formic acid, 60 °C, 24 h, 84 %; iii) TCEP·HCl, pH 7.0, RT, 1 h; iv) **12**, pH 6.5–7.0, RT, 16 h, 87 %; v) $GdCl_3 \cdot 6H_2O$, pH 7.0, RT, 24 h, 79 %.

nediaminetetraacetic acid (EDTA), a common Gd^{3+} chelator. The GdEDTA complex, excess of EDTA, and other impurities were finally removed by using a centrifugal filter unit with 3 kDa molecular weight cutoff (MWCO) and the dendrimeric complex **dMT3-CA** was used in subsequent studies. The dendrons **16** and **dMT3-CA** were also analyzed by means of MALDI-TOF MS showing again broad peaks with an average number of 19 DOTA chelators attached to the PAMAM G4 dendron, which is completely in line with results observed for the initial dendrimers **13** and **14** that have double the number of DOTA units (see above).

In summary, two new multimodal, targeted CAs were synthesized by coupling either a single (**mMT3-CA)** or dendrimer-linked (**dMT3-CA**) Gd^{3+} chelate, FITC, and biotin around a tripartite core. The loading efficiency of the dendrimer carrier was 60 %, thus generating a CA with 19 Gd^{3+} chelates per molecule.

Longitudinal relaxivity of monomeric and dendrimeric CAs

Longitudinal r_1 relaxivity values of **5**, **mMT3-CA**, and **dMT3-CA** were determined at 7 T (300 MHz) and 25 °C. The T_1 relaxation times were recorded at pH 7 in phosphate-buffered saline (PBS) at different concentrations of Gd^{3+}, prepared by diluting the stock solutions of **5**, **mMT3-CA**, and **dMT3-CA** with appropriate amounts of PBS. The exact concentration of Gd^{3+} in stock solutions was determined by the bulk magnetic susceptibility shift method.[15] The r_1 relaxivity of each CA was obtained as a slope of the linear regression curve for concentrations of Gd^{3+} plotted against relaxation rate (R_1). The r_1 values of (4.78 ± 0.10), (6.95 ± 0.10), and (6.08 ± 0.06) $mM^{-1}s^{-1}$ (calculated per mM of Gd^{3+}) were determined for **5**, **mMT3-CA**, and **dMT3-CA**, respectively.

Binding of targeted contrast agents to NeutrAvidin–agarose gel

To test the performance of the synthesized CAs, NeutrAvidin™–agarose gel was used as an in vitro model of target biological tissue. This material consists of NeutrAvidin, a variant of the avidin protein, immobilized onto beaded agarose. Solutions containing 1 mM of the targeted CA, as well as a commercially available nontargeted CA Dotarem®, were incubated with the beads. A fourth sample was incubated with PBS containing no CA, to control for any background signal resulting from the beads alone. The beads were washed to remove excess CA

and then analyzed by fluorescence measurements, MRI, and ICP-MS. The experiments were repeated in triplicate.

Fluorescence measurements and images

Contrast agent binding was verified by checking the beads for fluorescence of the FITC moiety ($\lambda_{ex}=485$ nm, $\lambda_{em}=520$ nm), which is present on both of the targeted CAs but not Dotarem. Beads treated with the targeted CA were fluorescent when placed on a blue light source and viewed through an amber filter (Figure 1, top). The beads that had been treated with the monomeric CA appeared brighter than those treated with the dendrimer. No fluorescence was observed with untreated beads or beads treated with Dotarem. Quantification of fluorescence signals in a multiplate reader revealed a similar trend. The intensity of beads treated with monomeric CA (**mMT3-CA**) was 3.6-fold greater than that for beads treated with the dendrimer (**dMT3-CA**; Figure 1, bottom, and Table 1). As expected, fluorescence intensities of both PBS- and Dotarem-treated beads were below background level. Overall, the fluorescence studies indicate that both targeted CAs bind efficiently and specifically to the target protein avidin. The quantitative data suggest a possible greater binding efficiency for the monomeric agent in comparison to the dendrimeric CA.

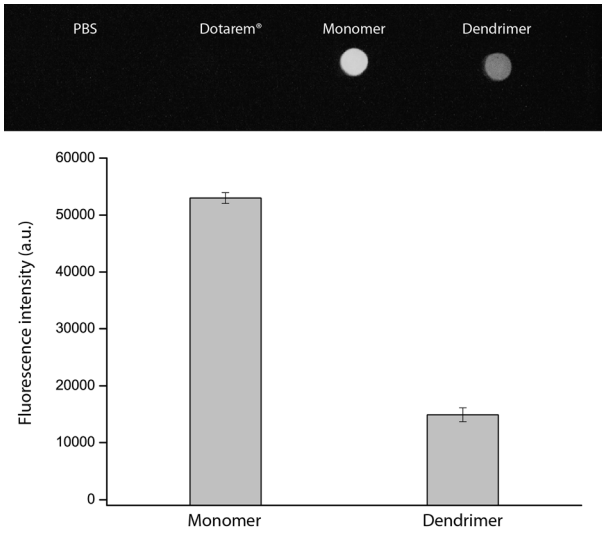

Figure 1. Fluorescence intensities of CA-treated NeutrAvidin–agarose gel measured in a microplate reader with excitation/emission filters appropriate for the FITC fluorophore ($\lambda_{ex}=485$ nm/$\lambda_{em}=520$ nm). Bar plots show the mean intensities of beads of three experiments ± standard deviation (SD). Top inset: fluorescence images of beads treated with PBS, Dotarem, **mMT3-CA**, and **dMT3-CA**.

Table 1. Analysis of CA binding to NeutrAvidin–agarose gel.[a]

Sample	Fluorscence intensity [a.u.][a]	T_{1w} MRI intensity (norm.)[b]	Relative Gd^{3+} content[a,b]	Ratio Gd^{3+}[a,c]
PBS	–	1.0	–	–
Dotarem	–	1.1	1.0	–
mMT3-CA	52965	1.9	11.2	–
dMT3-CA	14891	9.6	151.5	13.5

[a] Fluorescence intensity; reported results are means of three independent experiments. [b] As determined by ICP-MS. [c] Ratio of Gd^{3+} content of dendrimer/monomer (**dMT3-CA/mMT3-CA**).

T_1-weighted magnetic resonance imaging

Eppendorf tubes containing PBS-, Dotarem-, monomer-, or dendrimer-treated NeutrAvidin–agarose beads were imaged in the MRI scanner operating at 7 T. A set of T_1-weighted (T_{1w}) images was generated using a series of 30 repetition times (TRs) ranging from 21 to 8000 ms. For each set of parameters we acquired transverse and sagittal plane images at an in-plane resolution of 200 μm and slice thickness of 2 mm (Figure 2a, b). We visually inspected the set of transverse images, and performed region of interest (ROI) analysis (for details see

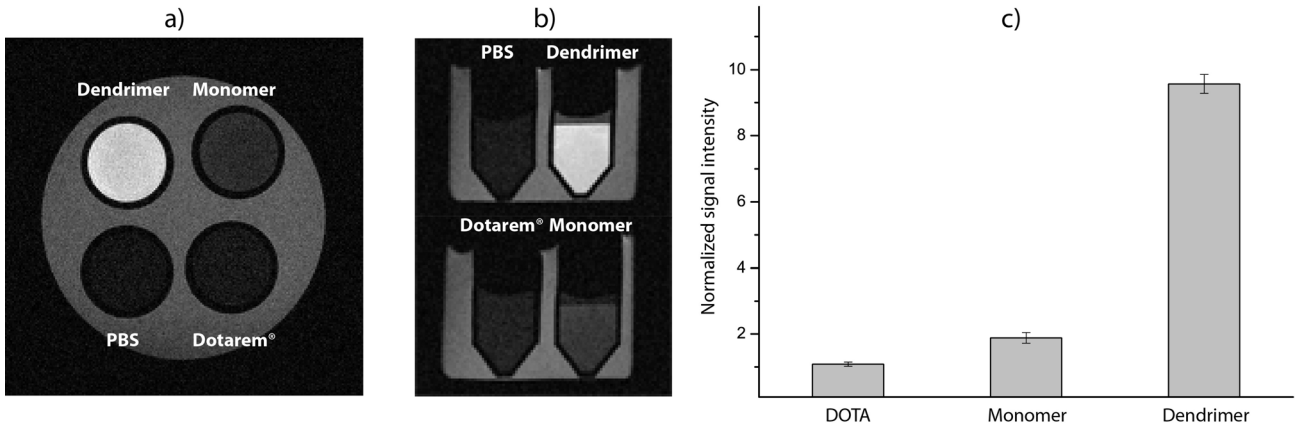

Figure 2. Representative transverse and sagittal plane T_{1w} MR images of NeutrAvidin–agarose gel treated with PBS, Dotarem, **mMT3-CA** (Monomer), or **dMT3-CA** (Dendrimer). Acquisition parameters: $B_0=7$ T, field of view = 4×4 cm (a) or 4×6 cm (b), matrix 200×200 (a) or 200×300 (b), slice thickness = 2 mm, echo time TE = 6 ms, TR = 58.5 ms. c) Plot showing the quantified T_{1w} signal intensity for each CA sample calculated from a dataset of images similar to (a), averaged from three replicate experiments and normalized to the PBS control. Bars indicate ± 1 SD.

the Experimental Section) to quantify the average pixel intensity of each sample. The signal intensities of the CA-treated samples varied depending on the TR used for image acquisition. The greatest signal change was found with the dendrimeric CA at TR = 59 ms; therefore, further analysis was performed on this dataset. Binding of the dendrimeric agent caused a nearly tenfold increase in bead signal intensity (Figure 2c). Binding of the monomer also led to a noticeable enhancement (about twofold). Dotarem treatment caused only a marginal increase (1.1-fold), which suggests a small degree of nonspecific bead retention of this nontargeted CA. In summary, binding of both monomeric and dendrimeric CA increased target contrast in T_{1w} images. Comparatively, the dendrimeric CA showed an overall increase in performance of approximately fivefold over the monomer.

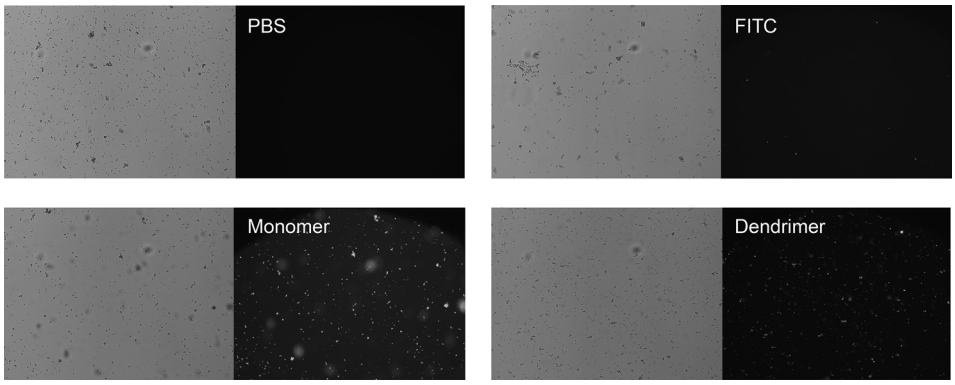

Figure 3. Microscopic analysis of 2 μm NeutrAvidin-coated polystyrene microspheres treated with PBS, FITC, **mMT3-CA** (Monomer), or **dMT3-CA** (Dendrimer). Left image shows the beads under bright-field illumination; right image with excitation/emission filters appropriate for the detection of the FITC fluorophore (λ_{ex} = 485 nm/ λ_{em} = 520 nm).

Inductively coupled plasma mass spectrometry analysis

The samples containing NeutrAvidin–agarose gel treated with PBS, Dotarem, **mMT3-CA**, or **dMT3-CA** were digested in concentrated HNO_3 to obtain the Gd^{3+} in the ionic form and its amount was determined by ICP-MS. The ICP-MS data were consistent with observations derived from the fluorescence and MRI studies (Table 1). Gadolinium was detectable in the three bead samples treated with Dotarem, monomer (**mMT3-CA**), or dendrimer (**dMT3-CA**). The nonspecific nature of the Dotarem interaction was indicated by much lower bead-associated Gd^{3+} in comparison to either of the targeted agents **mMT3-CA** and **dMT3-CA**. The beads treated with **dMT3-CA** were associated with approximately 14 times more Gd^{3+} relative to monomeric CA (Table 1). This is consistent with the dendrimer's determined approximately 19:1 content of GdDOTA/biotin but slightly lower binding to the NeutrAvidin–agarose gel (indicated by fluorescence experiments, see above).

Testing targeted CA for microscopic analysis of NeutrAvidin-coated microspheres

The functionality of the targeted CA was further assessed by fluorescence microscopy after binding to 2 μm spherical polystyrene microspheres displaying the target protein NeutrAvidin. The microspheres could be observed with a FITC-appropriate filter set following treatment with either of the targeted CAs (**mMT3-CA** or **dMT3-CA**) but not when treated with the nontargeted FITC fluorophore (Figure 3). Similar to other experiments described above, the fluorescence intensity of the monomer-treated targets was greater than that for those treated with the dendrimer. These data indicate that these two targeted MRI CAs (**mMT3-CA** and **dMT3-CA)** can additionally be used for imaging at the microscopic scale.

Discussion

The effectiveness of the developed synthetic strategy and the properties of the obtained products can be scrutinized through several aspects studied in the experiments described above. We synthesized bimodal, multivalent targeted CAs that can be detected through both optical fluorescence and MRI contrast signals. The synthetic route is based on the building block model, which allows easy replacement of the individual moieties. This strategy would allow easy modifications and potentially further improvements of the function of our targeted CAs. In this study we have initially coupled the core lysine molecule to biotin as a prototype ligand that binds specifically to the protein avidin. Depending on the desired target receptor, our approach allows implementation of versatile ligands that ensure the binding specificity.

Furthermore, we used a standard fluorescent dye FITC, which allows assessment of the targeted CA also by means of optical methods. Replacement of the dye with ones having more convenient optical properties that allow more thorough in vitro studies with cell cultures can now be performed in a straightforward and selective fashion. This is an additional advantage of our synthetic approach: common procedures with the multivalent carrier (dendrimers, nanoparticles) often involve nonspecific coupling of fluorescent dyes to the carrier surface without stoichiometric control. Herein, we report a procedure that ensures coupling of a single fluorescent unit to the desired targeted molecule, which can be very advantageous for various quantitative fluorescence assays.

Finally, in this approach we used G4 PAMAM dendron with maximally 32 surface coupling groups. Increasing the initial dendrimer generation can certainly lead to further MRI signal amplification. Targeted nanosized products with two different types of dendrons could be also prepared by following this strategy;[16] for instance, although a higher-generation dendron is used for MRI signal amplification, a lower-generation den-

dron could carry several ligands to improve the binding efficacy of the CA to its target.

The longitudinal r_1 relaxivities of all the studied Gd complexes (**5**, **mMT3-CA**, and **dMT3-CA**) are in line with previously studied low-, middle-, and high-molecular-weight complexes at high magnetic fields. As expected, a low-molecular-weight complex **5** has the lowest r_1 relaxivity. Despite the increase in their size, monomeric and dendrimeric CAs do not exhibit a dramatic increase in the r_1, which is probably a result of the magnetic field applied in this experiment (7 T).[17] Nevertheless, the $r_1 \approx 114$ mM^{-1}s^{-1} for **dMT3-CA** when calculated per dendrimer molecule (approximately 19 monomeric units with each $r_1 \approx 6$ mM^{-1}s^{-1}) suggests this CA could indeed be useful and utilized for signal amplification in targeted MRI approaches.

The targeting properties of the synthesized monomeric and dendrimeric CAs were studied by using various methods and types of targets. The agents exploit the high-affinity biotin–avidin interaction and were found to stably label avidin-coated microspheres and NeutrAvidin–agarose gel beads. The fluorescence microscopy experiments qualitatively exhibit stronger fluorescence intensity by monomeric **mMT3-CA** than dendrimeric **dMT3-CA**. Similarly, the fluorescence spectroscopy measurements resulted in 3.6-fold stronger fluorescence intensity of monomeric CA. Although a direct quantitative comparison of the binding cannot be performed because the emission properties of dye in the targeted molecule may change upon interaction with the protein, we conclude that **mMT3-CA** binds more efficiently than **dMT3-CA** most likely owing to the smaller size of the former.

On the other hand, we were able to show that MRI efficacy of the targeted CA can be substantially enhanced by generating a multivalent dendrimeric structure decorated with almost 20 Gd^{3+} ions per molecule. Despite weaker binding of **dMT3-CA** owing to its size, we observed an approximately tenfold MRI signal enhancement relative to a nonspecific and commercially available CA, Dotarem, and an approximately fivefold signal increase compared with **mMT3-CA**. These results can potentially be improved by increasing the dendron generation, incorporation of a longer spacer between the ligand and the rest of the dendrimeric molecule, or another dendron with increased valency for ligands. However, we note that increase in the MRI signal is not directly proportional to the local increase of Gd^{3+} concentration (achieved through higher dendrimer valency or binding efficiency), since the background MR signal also plays an important role and contributes to the recorded signal.

The results obtained from ICP-MS experiments could actually be the most directly linked to binding efficiency of our targeted CAs, thereby resolving the potential confusion generated by the discrepancy in signal quantifications obtained from fluorescence spectroscopy and MRI experiments. The Gd^{3+} amounts determined in various samples undoubtedly show a specific binding of **mMT3-CA** and **dMT3-CA** to NeutrAvidin–agarose gel, over Dotarem. Furthermore, the 13.5:1 ratio of Gd^{3+} content of dendrimer/monomer (**dMT3-CA**/**mMT3-CA**) suggests a less than two times weaker binding of dendrimer, given its 19 times higher Gd^{3+} content over the monomer.

Based on considerations discussed above, both CAs are expected to increase the MRI contrast of materials displaying the target protein. Greater gains are predicted for the dendrimeric agent as it carries multiple Gd^{3+} chelates per molecule and has a higher molecular relaxivity at relevant, high field strengths used in experimental research.

Extending the applications of the CAs described here, studies with 2 μm polystyrene microspheres suggest that they can also be used to image the target structure by using fluorescence microscopy. Therefore they could be used as true multimodal agents with improved range of spatial resolution. This is a valuable property as the features of MRI imaging (whole-body penetration, micrometer to centimeter spatial resolution, noninvasive) are highly complementary to those of fluorescence microscopic imaging (limited tissue penetration, nanometer to micrometer resolution, performed on fixed histological specimens). The use of a single multimodal agent combining both optical and MRI signaling capabilities allows for experiments employing both imaging approaches simultaneously.

The NeutrAvidin-coated polystyrene microspheres can also be considered as a good model of cells with a higher content of avidin expressed on their surface. Consequently, the specific binding of our targeted CAs envisages a number of diverse applications for these probes to investigate living systems. In one possible implementation, the polypeptide target avidin could be encoded as a transgene, manipulated using molecular biology, and introduced into living cells of model organisms. As shown previously, a fusion between avidin and a membrane-associated protein can be generated for expression on the outer surface of the cell as a receptor for targeted agents.[18] By deploying genetically engineered target receptors with the available strategies for spatiotemporal control of transgene expression (e.g., tissue-specific or inducible promoters), the corresponding CA could be used to study the development, physiology, or pathology of specific cell types and tissues in multimodal high-field MRI/optical experiments.

Conclusion

A new synthetic strategy for the preparation of target-specific multivalent contrast agents (CAs) has been developed. A bimodal biotinylated dendrimeric CA was prepared and its properties were compared with those of its monomeric analogue. Fluorescence-based studies proved the efficient binding of both monomeric and dendrimeric CAs to avidin-coated microspheres and agarose gel beads. Magnetic resonance imaging (MRI) experiments with avidin-coated agarose gel beads show remarkable signal enhancement of dendrimeric CAs, thus providing a promising application outlook for targeted CAs based on this approach. Used alone or in combination with appropriate nanosized carriers, we foresee new attempts in MRI of various cellular receptors and consequently specific cellular populations. This could lead to our better understanding of essential physiological and pathological processes and would be a great asset to the current clinical diagnostics or neuroimaging for understanding brain function.

Experimental Section

General remarks

All commercially available chemicals were used without further purification. DO3A-*t*Bu ester was purchased from Click Chemistry Technology, Beijing, China. D-Biotin and N_ε-Boc-L-lysine methyl ester hydrochloride were purchased from Sigma–Aldrich, Germany. FITC was purchased from Biomol, Germany. SMCC was purchased from Shangai YFan Chemistry Co., Ltd., Shanghai, China. Cys-PAMAM-G4 was purchased from Dendritic Nanotechnologies Inc., USA. *Tert*-Butyl 2-bromo-4-(4-nitrophenyl)butanoate was prepared according to the literature procedure.[19] FluoSpheres NeutrAvidin-labeled microspheres, 1.0 μm, nonfluorescent, were obtained from Molecular Probes Inc., Eugene, Oregon, USA. NeutrAvidin high-capacity agarose resin was purchased from Pierce Biotechnology, Rockford, USA.

^{1}H and ^{13}C NMR spectroscopy and relaxometric experiments were performed on a Bruker Avance III 300 MHz spectrometer, Germany. Fourier transform ion cyclotron resonance (FT-ICR) MS analysis was performed by a Bruker FT-ICR Apex II spectrometer, Germany. Electrospray ionization (ESI)-TOF-MS experiments were performed on MAXIS 3G spectrometer, Bruker Daltonics Inc., Germany. MALDI-TOF MS analysis was performed by The Scripps Center for Mass Spectrometry, La Jolla, CA, USA. ICP-MS experiments were performed by Currenta GmbH & Co. OHG, Leverkusen, Germany. Fluorescence microscopic imaging of microspheres was performed with an AxioImager.Z1 upright microscope (Zeiss, Germany) equipped with an AxioCamHR3 camera. Fluorescence imaging of agarose gel was performed using a Safelmager 2.0 blue (470 nm) LED source transilluminator (Life Technologies) and the supplied amber emission filter. Fluorescence intensity measurements were performed on a Fluostar Optima Plate Reader (BMG Labtech, Germany). The MR images were acquired at 21 °C using a 7 T Bruker BioSpec 70/30 USR Preclinical MRI system with a ^{1}H/volume transmit–receive coil tuned to the proton resonance (300.3 MHz).

Synthetic procedures

4-(4-Nitrophenyl)-2-(4,7,10-tris-*tert*-butoxycarbonylmethyl-1,4,7,10-tetraazacyclododec-1-yl)butyric acid *tert*-butyl ester (**1**): A suspension of tri-*tert*-butyl 2,2′,2″-(1,4,7,10-tetraazacyclododecane-1,4,7-triyl)triacetate (1.54 g, 3.02 mmol), *tert*-butyl 2-bromo-4-(4-nitrophenyl)butanoate (1.35 g, 3.92 mmol), and potassium carbonate (1.04 g, 7.54 mmol) in dimethylformamide (DMF, 10 mL) was prepared and stirred at 45 °C for 16 h. Dimethylformamide was removed under reduced pressure. The residue was dissolved in dichloromethane (200 mL) and extracted with water (2×200 mL). Dichloromethane was evaporated under reduced pressure and a brown amorphous solid product (2.25 g, 96%) was obtained by column chromatography (silica gel, 10% methanol/dichloromethane). ^{1}H NMR (300 MHz, $CDCl_3$): δ = 8.12 (d, J = 8.3 Hz, 2H; Ar*H*), 7.34 (d, J = 8.5 Hz, 2H; Ar*H*), 3.61–1.59 (overlapping m, 27H; CH_2 cyclen ring, ArCH_2CH_2C*H*COO*t*Bu and CH_2COO*t*Bu), 1.53 (s, 9H; (CH_3)$_3$C), 1.43 ppm (br, 27H; (CH_3)$_3$C); ^{13}C NMR (75 MHz, $CDCl_3$): δ = 174.9 172.8, 170.4 (*C*(O)), 149.1, 146.5, 129.6, 123.6 (Ar*C*), 82.4, 81.8 ((CH$_3$)$_3$*C*), 59.3 (*C*HCOO*t*Bu), 55.8, 55.5, 52.6, 52.4, 52.0 (CH_2 cyclen ring), 34.5 (ArCH_2CH_2), 28.1 (ArCH_2CH_2), 27.9, 27.8, 27.8 ppm ((CH_3)$_3$C); FT-ICR/HRMS: *m/z* calcd for $C_{40}H_{68}N_5O_{10}^+$: 778.4961 $[M+H]^+$; found: 778.4957.

4-(4-Aminophenyl)-2-(4,7,10-tris-*tert*-butoxycarbonylmethyl-1,4,7,10-tetraazacyclododec-1-yl)butyric acid *tert*-butyl ester (**2**): The nitrobenzene derivative **1** was dissolved in ethanol (10 mL) and Pd/C catalyst (300 mg) was added to the solution. The heterogeneous mixture was shaken for 16 h under a hydrogen atmosphere (30 psi) in a Parr hydrogenator apparatus. The catalyst was removed by filtration through Celite. The solvent was evaporated to obtain a brown amorphous solid compound (2.74 g, 95%). ^{1}H NMR (300 MHz, $CDCl_3$): δ = 6.86 (d, J = 8.2 Hz, 2H; Ar*H*), 6.59 (d, J = 8.3 Hz, 2H; Ar*H*), 3.55–1.65 (overlapping m, 27H; CH_2 cyclen ring, ArCH_2CH_2C*H*COO*t*Bu and CH_2COO*t*Bu), 1.63–1.25 ppm (br, 36H; (CH_3)$_3$C); ^{13}C NMR (75 MHz, $CDCl_3$): δ = 175.6, 172.8, 172.6 (*C*(O)), 145.1, 120.0, 129.6, 115.1 (Ar*C*), 81.8, 81.7, 81.6 ((CH$_3$)$_3$*C*), 58.2 (*C*HCOO*t*Bu), 55.7, 55.4, 52.5, 52.4, 51.6, 48.5, 48.3, 48.1, 47.0, 44.4 (CH_2 cyclen ring), 33.1 (ArCH_2CH_2), 28.2 (ArCH_2CH_2), 27.9, 27.8, 26.1 ppm ((CH_3)$_3$C); FT-ICR/HRMS: *m/z* calcd for $C_{40}H_{70}N_5O_8^+$: 748.5219 $[M+H]^+$; found: 748.5224.

4-(4-Isothiocyanatophenyl)-2-(4,7,10-tris-*tert*-butoxycarbonylmethyl-1,4,7,10-tetraazacyclododec-1-yl)butyric acid *tert*-butyl ester (**3**): Thiophosgene (7.83 mmol, 0.40 mL) was added to a mixture of **2** (2.67 mmol, 2.00 g) and triethylamine (1 mL) in dichloromethane (20 mL). The reaction mixture was stirred at room temperature for 24 h. The solvent was removed under reduced pressure, the crude product was purified by column chromatography (silica gel, 10% methanol/dichloromethane), and the product **3** was obtained as a light brown amorphous solid (1.49 g, 71%). ^{1}H NMR (300 MHz, $CDCl_3$): δ = 7.07 (s, 2H; Ar*H*), 3.51–1.56 (overlapping m, 27H; CH_2 cyclen ring, ArCH_2CH_2C*H*COO*t*Bu and CH_2COO*t*Bu), 1.55–1.28 ppm (br, 36H; (CH_3)$_3$C); ^{13}C NMR (75 MHz, $CDCl_3$): δ = 175.1, 172.8, 172.7 (*C*(O)), 140.4, 137.8, 129.9, 129.3, 125.6 (Ar*C*), 82.3, 81.9, 81.7, 81.6 ((CH$_3$)$_3$*C*), 58.8 (*C*HCOO*t*Bu), 55.8, 55.5, 55.4, 52.5, 52.4, 51.9, 48.5, 48.2, 47.1, 44.6 (CH_2 cyclen ring), 34.0 (ArCH_2CH_2), 27.9, 27.8, 25.8 ppm; FT-ICR/HRMS: *m/z* calcd for $C_{41}H_{68}N_5O_8S^+$: 790.4788 $[M+H]^+$; found: 790.4777.

4-(4-Nitrophenyl)-2-(4,7,10-tris-carboxymethyl-1,4,7,10-tetraaza-cyclododec-1-yl)butyric acid (**4**): The nitrobenzene derivative **1** (0.13 mmol, 100 mg) was dissolved in formic acid and the mixture was stirred at 60 °C for 16 h. Formic acid was evaporated under reduced pressure and the product was dried under high vacuum to give **4** as a light brown amorphous solid (67 mg, 94%). ^{1}H NMR (300 MHz, $CDCl_3$): δ = 8.16 (d, J = 8.4 Hz, 2H; Ar*H*), 7.48 (d, J = 8.4 Hz, 2H; Ar*H*), 4.04–2.64 (overlapping m, 25H; CH_2 cyclen ring, ArCH_2CH$_2$C*H*COO*t*Bu and CH_2COO*t*Bu), 2.18–1.82 ppm (br, 2H; ArCH$_2$CH_2CHCOO*t*Bu); ESI-LRMS: *m/z* calcd for $C_{24}H_{36}N_5O_{10}^+$: 554.2 $[M+H]^+$; found: 554.2.

Complex **5**: Macrocycle **4** (40 mg, 0.072 mmol) was dissolved in water and the pH was adjusted to 7.0 with aqueous sodium hydroxide (1 M). $GdCl_3{\cdot}6H_2O$ was added to the solution and the pH was maintained at 7.0 with the sodium hydroxide solution. The mixture was stirred at room temperature for 24 h. Chelex was added to the reaction mixture to remove excess Gd^{3+} ions. After filtration to remove Chelex, water was removed under reduced pressure to give a light brown solid product **5** (21 mg, 41%). ESI-TOF/HRMS: *m/z* calcd for $C_{24}H_{31}GdN_5O_{10}^-$: 707.1317 $[M-H]^-$; found: 707.1325.

6-*tert*-Butoxycarbonylamino-2-[5-(2-oxohexahydrothieno[3,4-*d*]imidazol-6-yl)pentanoylamino]hexanoic acid methyl ester (**6**): D-Biotin (3.37 mmol, 0.82 g), EDC·HCl (5.05 mmol, 0.97 g), and DMAP (8.42 mmol, 1.03 g) were dissolved in dimethylformamide (25 mL); H-Lys(Boc)-OMe (3.37 mmol, 1.00 g) was added to the mixture. The reaction mixture was stirred under nitrogen at room temperature for 48 h. The solvent was evaporated and the residue was poured into water (100 mL) and extracted with dichloromethane (3× 100 mL). The collected organic phases were dried over sodium sul-

fate and evaporated under reduced pressure. The crude product was purified by column chromatography (silica gel, 10% methanol/dichloromethane) to give **6** as a colorless amorphous solid (1.05 g, 64%). ^{1}H NMR (300 MHz, $CDCl_3$): δ = 4.86–4.68 (br, 1H; SCH_2CHNH), 4.57–4.40 (br, 1H), 4.37–4.22 (br, 1H), 3.71 (s, 3H; NHC*H*$COOCH_3$), 3.19–2.97 (br, 2H; CH_2NHCOO$(CH_3)_3$), 2.90 (dd, J = 12.8, 4.8 Hz, 1H; SCH_2CHNH), 2.71 (d, J = 12.8 Hz, 1H; SCH_2CHNH), 2.24 (br, 2H; CH_2C(O)NH), 1.86–1.56 (br, 6H; $CH_2CH_2CH_2$C(O)NHCHCH_2), 1.54–1.25 ppm (br, 15H; SCHCH_2 and $CH_2CH_2CH_2$NHCOOC$(CH_3)_3$); ^{13}C NMR (75 MHz, $CDCl_3$): δ = 173.9, 173.5, 164.4, 156.1 (*C*(O)), 79.0 ($(CH_3)_3C$), 61.9, 60.2, 55.9 (*C*H cyclen ring), 52.2 (NHCHCOOCH_3), 52.0 (NHCHCOOCH_3), 40.4, 40.1, 35.4, 31.4, 29.5 (-CH_2-), 28.4 ($(CH_3)_3C$), 28.2, 27.9, 25.4, 22.7 ppm (-CH_2-); ESI-TOF/HRMS: *m/z* calcd for $C_{22}H_{38}N_4NaO_6S^+$: 509.2404 $[M+Na]^+$; found: 509.2398.

{5-(2-Aminoethylcarbamoyl)-5-[5-(2-oxohexahydrothieno[3,4-*d*]imidazol-6-yl)pentanoylamino]pentyl}carbamic acid tert-butyl ester (**7**): Biotinylated lysine **6** (1.00 g, 2.06 mmol) was dissolved in methanol (10 mL); ethylenediamine (1 mL, 14.98 mmol) was added to the solution. The reaction mixture was kept at room temperature for 24 h. The crude product was washed with ethyl acetate to remove excess ethylenediamine and yield **7** as a colorless amorphous solid (0.81 g, 77%). ^{1}H NMR (300 MHz, $CDCl_3$): δ = 4.69–4.06 (br, 3H; SCH_2CHCH and NHC*H*C(O)NH), 3.85–2.68 (br, 9H; CH_2SCH, $NH_2CH_2CH_2NH$ and CH_2NHCOO), 2.45–2.00 (br, 2H; CH_2(CO)NH), 1.97–1.13 ppm (br, 21H; -CH_2- and $(CH_3)_3C$); ^{13}C NMR (75 MHz, $CDCl_3$): δ = 176.3, 174.9, 174.4, 165.1 (*C*(O)), 62.1, 60.7, 55.1 (*C*H cyclen ring), 54.5 (HNCHC(O)NH), 40.2, 40.0, 39.9, 37.2, 34.9, 30.7 (-CH_2-), 29.1 ($(CH_3)_3C$), 28.3, 27.5, 25.2, 22.6 ppm (-CH_2-); ESI-TOF/HRMS: *m/z* calcd for $C_{23}H_{43}N_6O_5S^+$: 515.3010 $[M+H]^+$; found: 515.3008.

Compound **8**: Biotinylated amine **7** (0.51 mmol, 0.26 g), fluorescein isothiocyanate (0.61 mmol, 0.24 g), and triethylamine (0.72 mmol, 0.10 mL) were dissolved in dimethylformamide (5 mL). The reaction mixture was stirred for 16 h at room temperature. The solvent was evaporated. The residue was purified by flash column chromatography (silica gel, gradient 10 to 20% methanol/dichloromethane) to yield **8** as an orange amorphous solid (0.40 g, 88%). ^{1}H NMR (300 MHz, CD_3OD): δ = 7.78 (d, J = 7.8 Hz, 1H; Ar*H*), 7.54 (s, 1H; Ar*H*), 7.15 (d, J = 8.2 Hz, 1H; Ar*H*), 6.92 (d, J = 8.6 Hz, 2H; Ar*H*), 6.66 (d, J = 2.4 Hz, 2H; Ar*H*), 6.57 (dd, J = 9.0, 2.5 Hz, 2H; Ar*H*), 4.50–4.40 (br, 1H; SCH_2CHCH), 4.32–4.16 (br, 2H; SCH_2CHCH and NHC*H*C(O)NH), 3.89–3.63 (br, 2H; $NHCH_2CH_2$NHC(S)NH), 3.56–3.32 (br, 3H; SC*H*CH and CH_2NHCOO$(CH_3)_3$), 3.18–3.07 (br, 1H; SC*H*), 2.87 (dd, J = 12.9, 5.0 Hz, 1H; SCH_2), 2.66 (d, J = 12.9 Hz, 1H; SCH_2), 2.35–2.12 (br, 2H; CH_2C(O)NHCHC(O)NH), 1.85–1.51 (br, 6H; -CH_2- and C$(CH_3)_3$), 1.50–1.27 ppm (br, 16H); ^{13}C NMR (75 MHz, CD_3OD): δ = 181.0 (*C*(S)), 174.4, 173.3, 169.7, 162.9 (*C*(O)), 159.9, 156.5, 152.6, 147.1, 140.3, 130.2, 128.9, 127.4, 124.3, 118.9, 112.5, 109.9, 102.4 (Ar*C*), 78.8 ($C(CH_3)_3$), 61.5, 61.4, 59.8, 55.1, 53.32, 43.6, 41.9, 39.8, 39.5, 38.4, 36.2, 34.8, 31.0, 28.9 (-*C*H- and -CH_2-), 27.8, 27.6, 27.5 ($(CH_3)_3C$), 25.0, 22.5 ppm (-CH_2-); ESI-TOF/HRMS: *m/z* calcd for $C_{44}H_{54}N_7O_{10}S_2^+$: 904.3368 $[M+H]^+$; found: 904.3378.

Compound **9**: Compound **8** (0.28 mmol, 0.25 g) was dissolved in methanol (5 mL) and concd HCl (5 mL) was added to this solution. The reaction mixture was kept at room temperature for 1 h. The solvent was evaporated under reduced pressure to give the product **9** (0.22 g, 97%). ^{1}H NMR (300 MHz, CD_3OD): δ = 8.15 (d, J = 6.4 Hz, 1H; Ar*H*), 7.64 (d, J = 9.2 Hz, 2H; Ar*H*), 7.44 (d, J = 8.3 Hz, 1H; Ar*H*), 7.38 (d, J = 2.1 Hz, 2H; Ar*H*), 7.23 (dd, J = 9.3, 2.1 Hz, 2H; Ar*H*), 4.63–4.49 (br, 1H; SCH_2CHCH), 4.45–4.17 (br, 2H; SCH_2CHCH and NHC*H*CONH), 4.08–3.67 (br, 2H; $NHCH_2CH_2$NHCSNH), 3.63–3.42 (br, 3H; SC*H*CH and CH_2NHCOO$(CH_3)_3$), 3.07–2.85 (br, 1H; SC*H*), 2.81–2.63 (br, 2H; SCH_2), 2.45–2.23 (br, 2H; CH_2CONHCHCONH), 2.09–1.38 ppm (br, 12H; -CH_2-); ^{13}C NMR (75 MHz, CD_3OD): δ = 183.2 (*C*(S)), 176.6, 175.1, 172.7, 167.8 (*C*(O)), 160.7, 143.7, 134.4, 132.7, 131.6, 127.9, 126.7, 121.2, 118.4, 103.5 (Ar*C*), 63.9, 62.4, 57.1, 55.2, 44.9, 41.1, 40.6, 40.5, 36.5, 34.7, 32.4, 29.8, 29.7, 29.5, 28.2, 26.8, 26.0, 24.2 ppm (-*C*H- and -CH_2-); ESI-TOF-MS: *m/z* calcd for $C_{39}H_{46}N_7O_8S_2^+$: 804.2844 $[M+H]^+$; found: 804.2839.

Compound **10**: The amine **9** (0.12 mmol, 0.10 mg), **3** (0.19 mmol, 0.15 mg), and triethylamine (0.36 mmol, 0.05 mL) were dissolved in dimethylformamide (5 mL); the reaction mixture was stirred at 45 °C for 16 h. The solvent was evaporated and the crude product was purified by column chromatography (silica gel, 20% methanol/dichloromethane) to give the orange product **10** (0.20 g, 68%). ^{1}H NMR (300 MHz, CD_3OD): δ = 8.27 (br, 1H; Ar*H*), 7.55–6.94 (br, 6H; Ar*H*), 6.92–6.38 (br, 6H; Ar*H*), 4.51–4.12 (br, 2H; SCH_2CHCH), 3.94–3.33 (br, 5H), 3.28–3.03 (br, 9H), 3.38–3.02 ppm (br, 20H); ^{13}C NMR (75 MHz, CD_3OD): δ = 183.0, 182.4 (*C*(S)), 177.1, 176.4, 175.2, 174.6, 171.2, 166.1, 162.0 (*C*(O)), 154.4, 142.3, 139.2, 138.7, 130.6, 129.5, 126.0, 125.7, 114.2, 111.8, 103.7 (Ar*C*), 82.3, 82.9, 82.8 ($(CH_3)_3C$), 63.3, 61.7, 59.5, 57.0, 56.9, 55.6, 55.5, 56.5, 55.2, 54.0, 53.9, 53.3, 45.4, 45.2, 41.2, 40.2, 40.1, 36.5, 32.7, 30.8, 29.8, 29.6, 29.4 (-*C*H- and -CH_2-), 28.6, 28.5, 28.4 (C$(CH_3)_3$), 26.9, 24.4, 24.1 ppm (-CH_2-); ESI-TOF/HRMS: *m/z* calcd for $C_{80}H_{113}N_{12}NaO_{16}S_3^{2+}$: 808.3723 $[M+H+Na]^{2+}$; found: 808.3722.

Compound **11**: Protected monomeric chelator **10** (0.085 mmol, 135 mg) was dissolved in formic acid (4 mL). The reaction mixture was stirred at 60 °C for 24 h. Formic acid was removed under reduced pressure to yield the orange product **11** (110 mg, 95%). ^{1}H NMR (300 MHz, D_2O): δ = ^{1}H NMR (300 MHz, D_2O): δ = 7.58–6.86 (br, 9H; Ar*H*), 6.74–6.45 (br, 4H; Ar*H*), 4.64–4.05 (br, 2H; SCH_2CHCH), 3.82–0.70 ppm (br, 51H; -*CH*- and -CH_2-); ESI-TOF/HRMS: *m/z* calcd for $C_{64}H_{81}N_{12}O_{16}S_3^+$: 1369.50501 $[M+H]^+$; found: 1369.50390; *m/z* calcd for $C_{64}H_{82}N_{12}O_{16}S_3^{2+}$: 685.2561 $[M+2H]^{2+}$; found: 685.2561.

mMT3-CA: The monomeric chelator **11** (82 mg, 60 μmol) was dissolved in water and the pH was adjusted to 7.0 with 0.1 M sodium hydroxide. $GdCl_3 \cdot 6H_2O$ (26 mg, 70 μmol) was added to the solution and the pH was maintained at 7.0 with the sodium hydroxide solution. The mixture was stirred at room temperature for 24 h. Chelex was added to the reaction mixture to remove excess Gd^{3+} ions. After filtration to remove Chelex, water was removed under reduced pressure to give the solid orange product **mMT3-CA** (46 mg, 51%). ESI-TOF/HRMS: *m/z* calcd for $C_{64}H_{76}GdN_{12}O_{16}S_3^-$: 1522.3920 $[M]^-$; found: 1522.3940.

Compound **12**: The amine **9** (100 mg, 0.12 mmol) was dissolved in PBS (pH 7.5). SMCC (20 mg, 0.60 mmol) was dissolved in dimethylformamide (0.5 mL) and added to the solution. The reaction mixture was stirred at room temperature for 4 h to give **12**. The product was used in the next step without further purification. ESI-LRMS: *m/z* calcd for $C_{51}H_{57}N_8O_{11}S_2^-$: 1021.4 $[M-H]^-$; found: 1021.4.

Compound **13**: Cys-PAMAM-G4 (45.2 mg, 3.12 μmol) was dissolved in dimethylformamide. Macrocycle **3** (240 mg, 0.30 mmol, 1.5 equiv according to dendrimer surface groups) and triethylamine (56 μL, 0.40 mmol) were added to the dendrimer. The reaction mixture was stirred at 45 °C for 48 h. The solvent was evaporated under reduced pressure and the residue was purified by lipophilic Sephadex column chromatography using methanol as eluent. The dark brown product **13** was obtained (165 mg, 81%). ^{1}H NMR (300 MHz, $CDCl_3$): δ = 7.49 (br, Ar*H*), 6.92 (br, Ar*H*), 4.38–1.56 (br), 1.56–

1.21 ppm (br, $(CH_3)_3C$); MALDI-TOF-MS: *m/z* calcd for $C_{2100}H_{3664}N_{430}Na_{45}O_{412}S_{39}^{2+}$: 21 880 $[M+45\,Na]^{2+}$; found: 21 876.

Compound **14**: The protected dendrimeric chelator **13** (180 mg, 3.45 μmol) was dissolved in formic acid (5 mL) and the mixture was stirred at 60 °C for 16 h. Formic acid was evaporated under reduced pressure and the product was freeze-dried to give **14** (120 mg, 84%). ^{1}H NMR (300 MHz, D_2O): $\delta = 7.23$ (br, Ar*H*), 4.45–0.40 ppm (br); MALDI-TOF-MS: *m/z* calcd for $C_{1524}H_{2512}N_{430}Na_{21}O_{412}S_{38}(H_2O)_{17}^{2+}$: 17 717 $[M+21\,Na+17\,H_2O]^{2+}$; found: 17 717.

Compound **15**: The dendrimeric chelator **14** (120 mg, 5.8 μmol) was dissolved in water. TCEP·HCl (16.63 mg, 58 μmol) was added and the pH was adjusted to 7.0 with 0.1 M sodium hydroxide solution. The reaction mixture was stirred at room temperature for 1 h. The reaction was monitored by TLC using Ellman's reagent. The appearance of a yellow spot confirmed the presence of thiol groups in **15**. The pH was then adjusted to 6.5–7.0 with hydrochloric acid. A solution of **12** was added to the reaction mixture and the pH was maintained at 6.5–7.0. The mixture was stirred at room temperature for 16 h. The unreacted dendron **15** was reoxidized by bubbling oxygen gas through the reaction mixture to give dendrimer **14**. Subsequently, the mixture was concentrated under reduced pressure and the excess amounts of **12** and dendrimer **14** were removed using a G-15 Sephadex column and water as eluent. Water was evaporated under reduced pressure and the product **16** was freeze-dried (110 mg, 87%). ^{1}H NMR (300 MHz, D_2O): $\delta = 7.21$ (br, Ar*H*), 4.09–0.51 ppm (br); MALDI-TOF-MS: *m/z* calcd for $C_{838}H_{1350}N_{228}Na_{16}O_{225}S_{22}(H_2O)_8^{2+}$: 19 347 $[M+16\,Na+8\,H_2O]^{2+}$; found: 19 347.

dMT3-CA: The dendronic chelator **16** (100 mg, 5.06 μmol) was dissolved in water and the pH was adjusted to 7.0 with 0.1 M sodium hydroxide. $GdCl_3{\cdot}6H_2O$ (90 mg, 243 μmol) was added to the solution and the pH was maintained at 7.0 with the sodium hydroxide solution. The mixture was stirred at room temperature for 24 h. EDTA (120 mg, 324 μmol) was added to the solution to remove excess Gd^{3+} while maintaining the pH at 7.0 with the aqueous sodium hydroxide solution. The mixture was stirred at room temperature for 24 h and the major part of GdEDTA and free EDTA was removed using water and a G-15 Sephadex column. The residues of GdEDTA and EDTA were removed by centrifugation with a 3 kDa centrifugal filter unit (102 mg, 79%). MALDI-TOF-MS: *m/z* calcd for $C_{838}H_{1274}Gd_{19}N_{228}Na_{37}O_{225}S_{22}(H_2O)_{37}^{2+}$: 11 676 $[M+37\,Na+37\,H_2O]^{2+}$; found: 11 676.

Binding of contrast agents to NeutrAvidin–agarose beads

Packed beads were incubated with 1 mM CA in PBS (0.01 M, pH 7.4) for 30 min at 4 °C with rotary shaking. Excess CA was removed and the beads were washed by repeated centrifugation and resuspension in PBS. After the final wash step, supernatant was removed and packed beads were kept for MRI scanning and subsequent analyses as described below.

MRI experiments

For MRI, 2 mL Eppendorf tubes containing NeutrAvidin–agarose bead/CA sample were placed in a 1% agar solution to avoid susceptibility distortions. Imaging was performed on a 7 T Bruker BioSpec 70/30 scanner, equipped with a BGA-12S gradient insert using a commercial quadrature volume resonator, Bruker 1H 112/086 QSN. For data acquisition a multislice–multiecho (MSME) spin–echo sequence was used for imaging. T_1-weighted saturation recovery MSME images were obtained with a series of varying repetition times and contrast, through the transverse and longitudinal planes of the sample tubes. Acquisition parameters were: field of view 4×4 cm^2, matrix 200×200, one axial 2 mm slice, TE = 6 ms, and TR = 21–8000 ms (logarithmic steps, 30 images). For longitudinal images the field of view was 4×6 cm^2, matrix 200×300, and two slices.

Processing of T_1-weighted MR images for display purposes: The 32-bit grayscale image files (2Dseq format) generated by the Bruker scanner Paravision software were opened using the ImageJ (v. 1.47d, Fiji package) image processing software. The images were converted to 8-bit files using the "Image-Type-8-bit" command and saved as TIFF format. The TIFF images were opened with Adobe Photoshop CS5 and rotated 90° clockwise.

Quantitative analysis of T_1-weighted MR images: The original T_{1w} images generated by the Paravision software (32-bit, 2Dseq format image files) were opened in the ImageJ (v. 1.47d, Fiji package) analysis software. A circular ROI was placed manually around each bead/CA sample outlining the largest possible diameter fitting within the walls of the sample tube, to maximize the number of pixels sampled for calculation (1000–1500 pixels). The ImageJ function "Analyze-Measure" was used to calculate the mean pixel intensity and total number of pixels within the ROI. Mean pixel intensities were exported into spreadsheets for further analysis.

Fluorescence intensity measurements

Equal volumes of CA-treated NeutrAvidin–agarose beads were placed in a 96-well plate and fluorescence intensities were measured in a FluoStar Optima microplate reader (BMG Labtech, Germany).

Fluorescence images of CA-treated NeutrAvidin–agarose beads: Fluorescence imaging was performed by placing the beads on a Safelmager 2.0 blue (470 nm) LED source transilluminator equipped with the supplied amber emission filter. Images were captured with a digital camera and cropped around a region containing the samples by using Photoshop CS5 software.

ICP-MS determination of Gd^{3+} associated with CA-treated NeutrAvidin–agarose beads

Equal volumes of the CA-treated NeutrAvidin–agarose samples were digested with 26% nitric acid at 50 °C for 72 h to release chelated Gd^{3+} into solution. The Gd^{3+} concentration was quantified by ICP-MS at Currenta GmbH & Co. (Leverkusen, Germany).

Fluorescence microscopy

Microscopic images were acquired using the AxioImager.Z1 upright microscope (Zeiss) equipped with an AxioCamHR3 (Zeiss) camera. Images were acquired over identical exposure times across all samples and exported as 16-bit grayscale, 1388×1040 pixel TIFF format files.

Acknowledgements

We thank Dipl. Ing. Michael Beyerlein for help in performing MRI experiments. Financial support from the Max-Planck Soci-

ety, the Turkish Ministry of National Education (PhD fellowship to S.G.), and European COST CM1006 and TD1004 Actions is gratefully acknowledged.

Keywords: chelates · contrast agents · dendrimers · gadolinium · imaging agents

[1] a) C. T. Yang, K. H. Chuang, *MedChemComm* **2012**, *3*, 552 – 565; b) G.-P. Yan, L. Robinson, P. Hogg, *Radiography* **2007**, *13*, e5 – e19; c) C. F. G. C. Geraldes, S. Laurent, *Contrast Media Mol. Imaging* **2009**, *4*, 1 – 23.

[2] a) A. E. Merbach, E. Toth, *The Chemistry of Contrast Agents in Medical Magnetic Resonance Imaging*, Wiley, Chichester, **2001**; b) R. B. Lauffer, *Chem. Rev.* **1987**, *87*, 901 – 927.

[3] G. E. Hagberg, I. Mamedov, A. Power, M. Beyerlein, H. Merkle, V. G. Kiselev, K. Dhingra, V. Kubiček, G. Angelovski, N. K. Logothetis, *Contrast Media Mol. Imaging* **2014**, *9*, 71 – 82.

[4] a) S. Aime, A. Barge, C. Cabella, S. G. Crich, E. Gianolio, *Curr. Pharm. Biotechnol.* **2004**, *5*, 509 – 518; b) K. Hanaoka, A. J. M. Lubag, A. Castillo-Muzquiz, T. Kodadek, A. D. Sherry, *Magn. Reson. Imaging* **2008**, *26*, 608 – 617.

[5] H. Kobayashi, S. Kawamoto, T. Saga, N. Sato, T. Ishimori, J. Konishi, K. Ono, K. Togashi, M. W. Brechbiel, *Bioconjugate Chem.* **2001**, *12*, 587 – 593.

[6] G. Gambino, J. Engelmann, L. Tei, M. Botta, N. K. Logothetis, I. Mamedov, *Biomaterials* **2013**, *34*, 7135 – 7142.

[7] M. D. Melamed, N. M. Green, *Biochem. J.* **1963**, *89*, 591 – 599.

[8] R. Mishra, W. Su, R. Pohmann, J. Pfeuffer, M. G. Sauer, K. Ugurbil, J. Engelmann, *Bioconjugate Chem.* **2009**, *20*, 1860 – 1868.

[9] a) M. Longmire, P. L. Choyke, H. Kobayashi, *Curr. Top. Med. Chem.* **2008**, *8*, 1180 – 1186; b) E. C. Wiener, M. W. Brechbiel, H. Brothers, R. L. Magin, O. A. Gansow, D. A. Tomalia, P. C. Lauterbur, *Magn. Reson. Med.* **1994**, *31*, 1 – 8; c) G. Yan, C. Ai, L. Li, R. Zong, F. Liu, *Chin. Sci. Bull.* **2010**, *55*, 3085 – 3093; d) M. Polasek, P. Hermann, J. A. Peters, C. F. G. C. Geraldes, I. Lukes, *Bioconjugate Chem.* **2009**, *20*, 2142 – 2153; e) S. Langereis, A. Dirksen, T. M. Hackeng, M. H. P. van Genderen, E. W. Meijer, *New J. Chem.* **2007**, *31*, 1152 – 1160; f) M. A. Bruckman, X. Yu, N. F. Steinmetz, *Nanotechnology* **2013**, *24*, 462001.

[10] a) S. Venkataraman, Z. A. Chowdhury, A. L. Lee, Y. W. Tong, I. Akiba, Y. Y. Yang, *Macromol. Rapid Commun.* **2013**, *34*, 652 – 658; b) C. A. Boswell, P. K. Eck, C. A. S. Regino, M. Bernardo, K. J. Wong, D. E. Milenic, P. L. Choyke, M. W. Brechbiel, *Mol. Pharmaceut.* **2008**, *5*, 527 – 539.

[11] D. A. Tomalia, B. Huang, D. R. Swanson, H. M. Brothers, J. W. Klimash, *Tetrahedron* **2003**, *59*, 3799 – 3813.

[12] H. Xu, C. A. S. Regino, Y. Koyama, Y. Hama, A. J. Gunn, M. Bernardo, H. Kobayashi, P. L. Choyke, M. W. Brechbiel, *Bioconjugate Chem.* **2007**, *18*, 1474 – 1482.

[13] G. Mattson, E. Conklin, S. Desai, G. Nielander, M. D. Savage, S. Morgensen, *Mol. Biol. Rep.* **1993**, *17*, 167 – 183.

[14] H. Xu, C. A. S. Regino, M. Bernardo, Y. Koyama, H. Kobayashi, P. L. Choyke, M. W. Brechbiel, *J. Med. Chem.* **2007**, *50*, 3185 – 3193.

[15] D. M. Corsi, C. Platas-Iglesias, H. van Bekkum, J. A. Peters, *Magn. Reson. Chem.* **2001**, *39*, 723 – 726.

[16] C. R. DeMattei, B. H. Huang, D. A. Tomalia, *Nano Lett.* **2004**, *4*, 771 – 777.

[17] J. B. Livramento, C. Weidensteiner, M. I. M. Prata, P. R. Allegrini, C. Geraldes, L. Helm, R. Kneuer, A. E. Merbach, A. C. Santos, P. Schmidt, E. Toth, *Contrast Media Mol. Imaging* **2006**, *1*, 30 – 39.

[18] a) S. Lehmann, E. G. Garayoa, A. Blanc, R. Keist, R. Schibli, M. Rudin, *J. Nucl. Med.* **2011**, *52*, 445 – 452; b) P. Lehtolainen, T. Wirth, A. K. Taskinen, P. Lehenkari, O. Leppanen, M. Lappalainen, K. Pulkkanen, A. Marttila, V. Marjomaki, K. J. Airenne, M. Horton, M. S. Kulomaa, S. Yla-Herttuala, *Gene Ther.* **2003**, *10*, 2090 – 2097; c) T. Mäntylä, J. M. Hakumaki, T. Huhtala, A. Narvanen, S. Yla-Herttuala, *Magn. Reson. Med.* **2006**, *55*, 800 – 804; d) F. Pinaud, X. Michalet, G. Iyer, E. Margeat, H. P. Moore, S. Weiss, *Traffic* **2009**, *10*, 691 – 712; e) F. Pinaud, D. King, H. P. Moore, S. Weiss, *J. Am. Chem. Soc.* **2004**, *126*, 6115 – 6123.

[19] S. M. Vibhute, J. Engelmann, T. Verbić, M. E. Maier, N. K. Logothetis, G. Angelovski, *Org. Biomol. Chem.* **2013**, *11*, 1294 – 1305.

Received: September 22, 2014
Published online on December 12, 2014